

## *Chapter 1*

# **Introduction**

Adapted from: Barton, J. K., Furst, A. L., and Grodick, M. A. (2015) DNA Sensors using DNA Charge Transport Chemistry, in DNA in Supramolecular Chemistry and Nanotechnology, 1<sup>st</sup> Ed. Wiley & Sons *In Press*.

and Furst, A. L., Hill, M. G., and Barton, J. K. (2014) Electrocatalysis in DNA Sensors, *Polyhedron* 84, 150-159.

## DNA Charge Transport

From the first proposal of the structure of DNA,<sup>1,2</sup> debates about what properties DNA may hold beyond the simple transfer of genetic information have arisen. The structure of the stacked DNA bases within the double helix led many to predict that this macromolecular assembly could conduct charge. The stacked base pairs closely resemble the structure of graphene sheets, as both contain aromatic heterocycles stacked at 3.4 Å (Figure 1.1).<sup>3</sup> However, the notion that the DNA helix can conduct charge was long met with skepticism. Today, as a result of extensive experimentation, DNA charge transport (DNA CT) is well-established chemistry, though the full mechanistic understanding still requires development.<sup>4</sup>

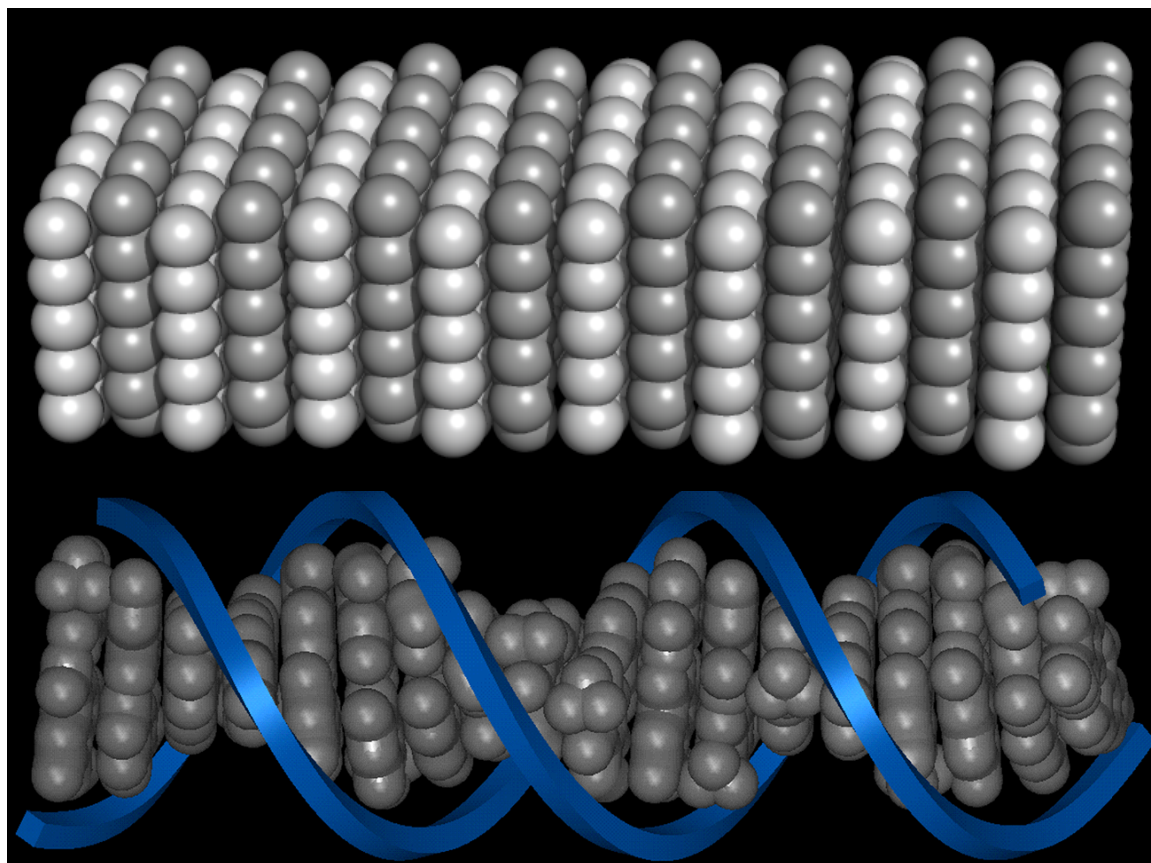


**Figure 1.1** Schematic illustrations of the structures of graphene (top) and DNA (bottom). The planar sheets of graphene are shown in grey, as are the aromatic DNA bases; for the DNA, the sugar-phosphate backbone has been schematized as a ribbon (blue). In both cases, the layers are stacked at a distance of 3.4 Å, enabling orbital overlap, and therefore the flow of charge.

Experiments with DNA CT first involved the observation of long-range, excited-state charge transport through a DNA duplex between well-stacked donors and acceptors.<sup>5-7</sup> In an early experiment, electron transfer between covalently tethered metallointercalators was observed over a distance of 40 Å through DNA (Figure 1.2).<sup>5</sup> A 15-base DNA duplex was labeled at one terminus with  $[\text{Ru}(\text{phen})_2\text{dppz}]^{2+}$  (dppz = dipyrido[3,2-*a*:2',3'-*c*]phenazine), with the excited state acting as an electron donor, and  $[\text{Rh}(\text{phi})_2\text{phen}]^{3+}$  (phi = 9,10-phenanthrenequinone diimine) at the opposite terminus acting as an electron acceptor. In the absence of the electron acceptor, the ruthenium complex tethered to DNA luminesces. However, upon incorporation of the rhodium complex, the luminescence is completely quenched. In the years since this experiment, the ability of DNA to conduct charge through its  $\pi$ -stacked bases has been studied extensively using a variety of platforms.<sup>5, 8-12</sup> Moreover, as the power of this chemistry became apparent, experiments focused on biological applications of DNA CT chemistry came to the forefront.<sup>13</sup>

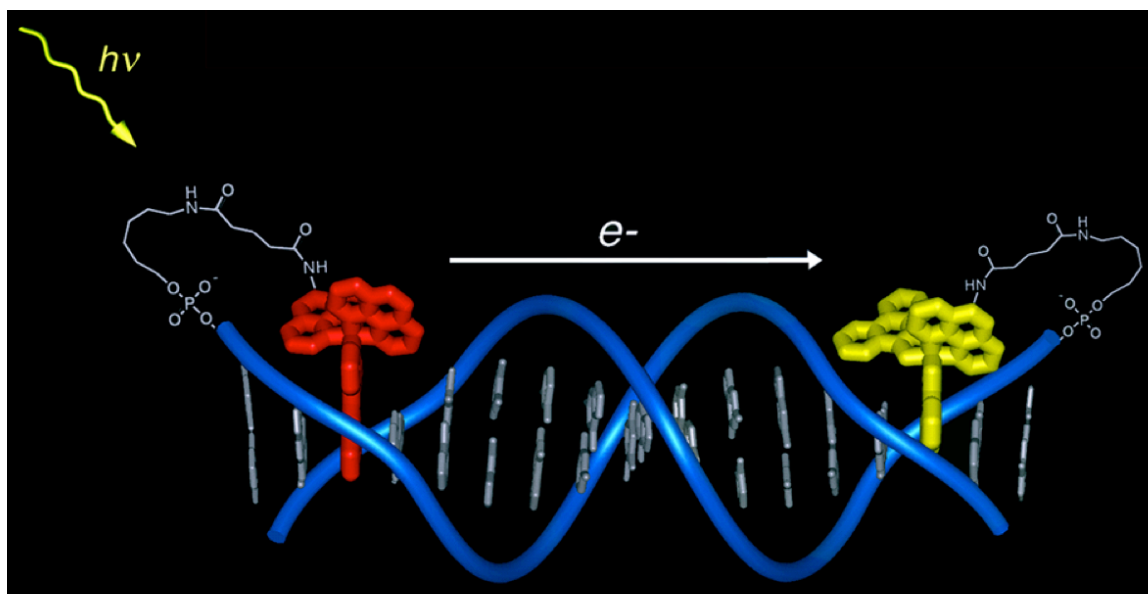


**Figure 1.2** A DNA modified with two metallobases to test photoinduced DNA CT. Electron transfer over 40 Å was shown through DNA between covalently tethered metallobases,  $[\text{Ru}(\text{phen})_2\text{dppz}]^{2+}$  (red) as an electron donor and  $[\text{Rh}(\text{phen})_2\text{phen}]^{3+}$  (yellow) at the opposite terminus as an electron acceptor.<sup>5</sup>

The remarkable utility of this chemistry became evident as DNA CT was shown to be extremely efficient over long molecular distances on fast time scales, yet exquisitely sensitive to perturbations in base-base stacking.<sup>14</sup> Single base mismatches and other damaged products have been shown to significantly attenuate CT both in ground and excited state experiments.<sup>15-17</sup> DNA CT has also been directly measured in single molecule experiments in the ground state.<sup>18</sup> Using an oxygen plasma, molecular size gaps can be inserted into carbon nanotubes and individual DNA molecules functionalized with terminal amines covalently attached within the gaps using amide chemistry. These robust devices can then be used to measure the current flow in the nanotube containing the covalently attached molecule of interest versus that current in the original nanotube (Figure 1.3). In these devices, duplex DNA was attached either by functionalizing the 5'-end of both strands of the DNA with alkyl amines or both 3'- and 5'-ends of only one of the strands of the duplex, with the complementary strand non-covalently associated. Using this device, we found that the resistance generated in the gap with a DNA duplex inserted was quite similar to that expected for a stacked graphite insert (~ 1 megaohm resistance for a ~6 nm gap).

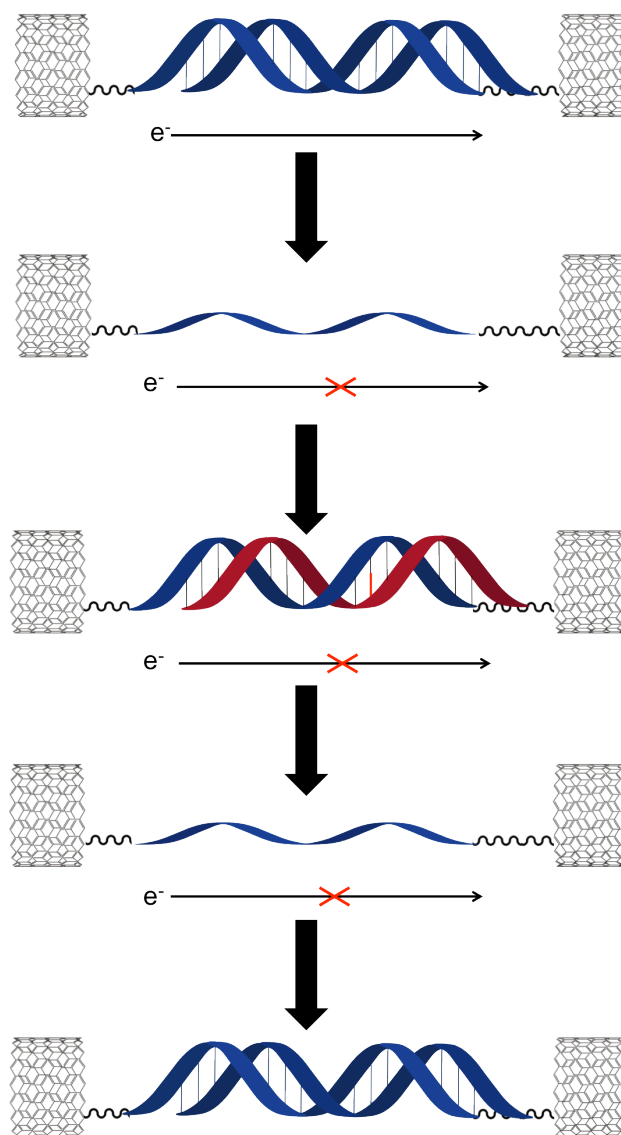


**Figure 1.3** Illustration of a single molecule experiment with DNA tethered to carbon nanotubes to test ground state DNA CT.<sup>18</sup> Well matched DNA is covalently attached to carbon nanotubes through the termini of the DNA functionalized with amines. The DNA can then be denatured in the device so that only one strand remains covalently attached. A complementary strand that contains a single base mismatch can then be floated in and annealed to the covalently tethered strand. For the well matched duplex DNA (top), significant current is obtained, but this current is attenuated in the presence of a mismatch (middle with red mismatch); addition of the well matched complement (bottom) restores full current flow. This cycle of unannealing and reannealing alternative complements can be repeated and the conductivity reproducibly measured.

Even more interesting was how this assembly could be used to test the effect of a mismatch on DNA CT. With one strand covalently attached to the device through both the 5'- and 3'-ends, various complements, with or without a mismatch, could be interchanged into the duplex and the resultant current tested (Figure 1.3). Several different complements could be cycled in this robust device. The presence of a mismatch was found to yield a 300-fold attenuation in current relative to the current found for the well matched complement. Moreover, all current was lost upon DNA cleavage with a blunt-end restriction enzyme, illustrating that the conformation of the DNA duplex in the gap was intact and recognizable by the DNA-binding protein.

While early experiments focused on the distance dependence of DNA CT using largely spectroscopic experiments involving excited state transport, ground state measurements repeatedly illustrated the high sensitivity of DNA CT to intervening perturbations in stacking.<sup>11</sup> Although the shallow distance dependence of DNA CT was remarkable, so too was the exquisite sensitivity of DNA CT to perturbations in base stacking. This led to significant applications of DNA CT chemistry in bio-sensing. DNA CT has allowed the sensitive detection of a variety of biologically relevant targets, including single base mismatches irrespective of sequence context, the monitoring of binding of DNA transcription factors, and even following, electrochemically, the reactions of various enzymes on DNA. DNA CT-based platforms represent one example within a broad family of nucleic acid sensing platforms.



## Nucleic Acid Biosensing

Detection of biologically relevant targets is vital for both fundamental research as well as clinical and field diagnostics. Sensing strategies that feature biological substrates for analyte capture provide a natural foundation for bioassays owing to the inherent molecular-recognition nature of substrate-ligand binding. Nucleic-acid-based platforms in particular comprise an especially robust and flexible class of sensors capable of detecting a variety of small-molecule, protein, and DNA/RNA targets.<sup>19</sup> Among the many different read-out strategies employed for DNA-based sensing (*e.g.*, fluorescence,<sup>20-23</sup> changes in conductivity,<sup>24, 25</sup> or mass<sup>26-30</sup> that accompany hybridization, *etc.*), we have focused on electrochemical methods.<sup>31, 32</sup> Electrochemical instrumentation is both low cost and portable, making this method of detection ideal for clinical diagnostics.

One of the first DNA electrochemical detection strategies involved the direct reduction of nucleic acid bases adsorbed onto a mercury electrode: hybridization of a target sequence increased the amount of adsorbed DNA, resulting in greater signals.<sup>33</sup> Similarly, sinusoidal voltammetry was used to measure the direct oxidation of the amine-containing nucleobases as well as the sugar-phosphate backbone of all nucleotides.<sup>34</sup> While this platform is potentially capable of detecting zeptomoles of DNA, it is impractical for biosensor applications due to its lack of specificity to differentiate between dissimilar sequences of DNA.

Alternative systems typically rely on indirect detection schemes, in which a redox-active mediator is employed either to report on the composition of target DNA or to induce redox reactions of the bases themselves.<sup>35</sup> Often, the target DNA is labeled with

a small, electrochemically active molecule; hybridization is then signaled by the appearance of an electrochemical signal. This technique mimics common fluorescence-based techniques in that the target, rather than the probe, is modified.<sup>36</sup> Target labeling has the advantage of presenting a ‘signal on’ method of detection—a hybridization event must successfully occur for an electrochemical signal to appear—yet is ultimately limited by the thermodynamic stability of the DNA duplexes formed. Non-specific hybridization can result in false positive signals, making the identification of subtle sequence variants, *e.g.*, single-nucleotide polymorphisms, impractical.

The probe sequence can also be labeled in electrochemical DNA sensors. One such system involves the application of a hairpin DNA construct as the probe molecule.<sup>37</sup> Hairpins are DNA architectures that are composed of a stem region containing a self-complementary sequence and a disordered loop region containing the target sequence. Upon hybridization to a complementary target, the hairpin opens. If the terminus of the stem region is modified with a redox-active moiety, the probe will be in close proximity to the surface in the hairpin form where it will be electrochemically active with no target bound. This signal will significantly diminish upon target binding.<sup>38</sup>

Finally, there are DNA-based electrochemical detection methods based on DNA ‘sandwich’ assemblies. These structures involve three sequences of DNA: a target molecule, a probe molecule tethered to the surface, and a reporter sequence.<sup>39-42</sup> The reporter sequence binds to an overhang of the probe-target duplex and can either directly generate an electrochemical signal or can be a component of an ancillary redox cycle. This method of detection negates the necessity of target labeling and maintains a ‘signal on’ detection scheme.

## **DNA-functionalized Electrochemical Sensors**

The most common technique employed for electrochemical detection based on DNA CT involves the immobilization of duplexed DNA on a gold surface at one terminus and modified with a redox-active probe at the distal terminus (Figure 1.4). A range of redox-active probes have been employed, and, unsurprisingly, the most sensitive reporters of the integrity of the DNA duplex are those that are themselves well stacked and hence well coupled into the DNA  $\pi$ -stack.

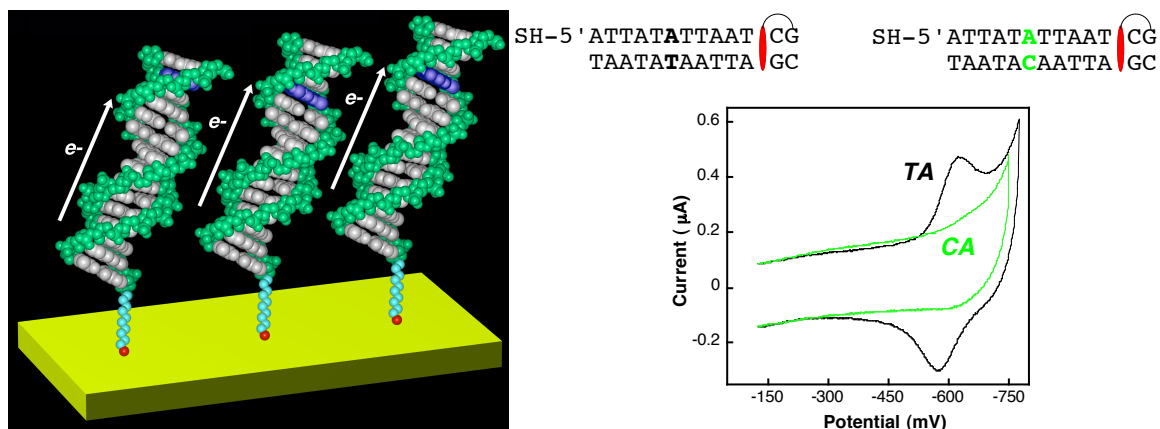


**Figure 1.4** Electrochemical signal from well matched DNA and DNA containing a single-base mismatch using DNA-modified electrodes. DNA assembled on a gold electrode (left) containing a covalent redox reporter daunomycin was electrochemically monitored by cyclic voltammetry (right).<sup>43</sup> The well matched DNA produces a large, reversible signal. Upon incorporation of a single-base mismatch, the electrochemical signal is significantly attenuated.

In one electrochemical experiment, the DNA duplex was shown to carry out ground state charge transport over 100 base pairs, or 34 nm.<sup>44</sup> This experiment involved a particularly long molecular wire, but the extraordinary sensitivity of DNA to small perturbations in the base stack was demonstrated through the significant electrochemical effect of a single mismatched base incorporated into the DNA duplex. The 100-mer was terminally modified with a covalent Nile blue redox probe and assembled on the gold electrode. The incorporation of a single mismatched base pair resulted in a significant attenuation of signal,  $0.8 \pm 0.1$  nC for the cathodic peak containing a single base mismatch, as compared to  $1.7 \pm 0.1$  nC for that of the well-matched duplex.<sup>44</sup> Interestingly, the degree of signal attenuation observed through 100 base pairs for the single base mismatch was equal to that observed for the same mismatch incorporated into a 17-mer. Remarkably, while the effect of the mismatch is substantial and independent of duplex length and sequence context, no perturbation in current is observed with a nick in the DNA backbone. The 100-mer used in this experiment was actually constructed from the annealing of several smaller pieces of DNA containing sticky ends. What is essential for DNA CT is effective base stacking; CT is through the base pair stack, not the sugar-phosphate backbone.

## **DNA-modified Electrode Formation**

Generally, a major challenge of DNA-based electrochemical sensors is the ability to detect bulky biomolecules specifically at a solid surface. Conventionally, DNA-modified electrodes are formed through the self-assembly of thiolated DNA onto a planar gold electrode.<sup>45</sup> However, this method provides only limited control over the spacing and total amount of DNA assembled on a surface. It has been shown, in fact, that DNA assembled in this manner clusters into regions of extremely high DNA density, leaving other areas on the electrode surface bare.<sup>46, 47</sup> This inhomogeneity can lead to issues with effective and consistent detection, as different regions of the electrode surface respond differently to the addition of analyte.<sup>48</sup> Additionally, upon inclusion of a shielding ion, such as  $\text{MgCl}_2$ , which neutralizes the negatively charged DNA backbone, DNA forms a fairly uniform but extremely dense monolayer. This type of morphology limits the access of targets to the surface probes, significantly decreasing the sensitivity of detection.<sup>49</sup> One major area of research, therefore, has been the development of methods to both better control the homogeneity of DNA-modified surfaces, as well as to increase the spacing between individual DNA helices. There are two main schools of thought as to how best to control the assembly of DNA helices: controlling the underlying electrode morphology through nanostructuring and attachment of DNA to pre-formed monolayers.

### ***Nanostructured Microelectrodes***

Nanostructured microelectrodes have been reported to yield better spacing of the DNA over conventional, planar electrodes by increasing the deflection angle between the DNA helices.<sup>50, 51</sup> Nanostructuring microelectrodes involves the preliminary formation

of patterned electrodes using conventional lithographic techniques onto a substrate. Subsequently, electrodeposition onto these pre-formed electrodes enables the formation of nanoscale structures that increase the overall surface area available for biomolecule attachment.<sup>52</sup> Multiple conditions for the addition of the nanostructured electrodes have been attempted, and small variations in the assembly conditions greatly affect the roughness of the resulting structures.<sup>53</sup> For example, applying higher deposition potentials leads to more highly patterned nanostructures, which reportedly enable greater access to individual DNA helices than their smooth counterparts. One consequence of the electrodeposition method, however, is that while the degree of patterning and the total amount of metal added can be controlled, the specific surface structure cannot. Thus, no two electrodeposited electrode surfaces will be identical, making direct comparisons potentially problematic.

Electrochemical detection with this platform involves the well known electrocatalytic signal amplification of  $\text{Fe}(\text{CN})_6^{3-}$  reduction mediated by the electrostatic reporter  $\text{Ru}(\text{NH}_3)_6^{3+}$ . Detection limits for hybridization assays using this technique have reached sub-femtomolar limits.<sup>53</sup> While this method of detection provides significant amplification, like all methods in which the electrochemical signals are monitored at the probe-modified surface, it also produces a large background signal, with relatively small electrochemical differentials between no hybridization to the target and full hybridization. While these small differentials can be translated into large percentage differentials, they have not yet been shown to be sufficiently reliable for clinical detection from crude samples.

### ***Controlled Self-Assembly onto Flat Surfaces***

Straightforward chemical methods can also be used to regulate the placement of DNA on planar electrodes and effectively control the homogeneity and spacing of the DNA duplexes within a sensing monolayer. Conventional DNA-modified electrode surfaces are formed through the self-assembly of thiolated DNA duplexes on gold surfaces. Owing to the restricted access of target molecules to sterically congested probe sequences, these monolayers are not ideal for the detection of large proteins, proteins that bind to specific sequences of DNA, or hybridization events. Although the surface density of the DNA monolayer can be controlled through the adjustment of the composition and ionic strength of the deposition solution—high ionic strength provides better Debye screening of the negative charges on DNA, enabling the DNA helices to pack closer together—the range of DNA surface coverages is narrow ( $\sim 40 - 50 \text{ pmol/cm}^2$ ). Similarly, conventional DNA assembly methods do not allow control over the homogeneity of DNA dispersed within a multicomponent film. It is also known that thiol-modified DNA forms a heterogeneous monolayer when combined with a passivating agent such as mercaptohexanol. The DNA helices cluster into large domains of very high density, leaving large regions of the surface almost entirely devoid of DNA.<sup>46, 47</sup> This helix clustering is especially problematic for detection because it leads to variability across the electrode surface and makes access to specific base sequences difficult.

An alternative method of monolayer formation, based on azide/alkyne “click” coupling, provides significantly more control over both the homogeneity of DNA within a monolayer and the total amount of DNA assembled onto the surface. With this



assembly technique, alkyne-labeled DNA is coupled to a pre-formed mixed alkanethiol monolayer doped with azide-terminated functionalities. The underlying composition of the monolayer determines the bulk DNA loading onto the film. Shown in Figure 1.5 is a schematic representation of the difference in spacing between DNA helices formed by thiolated DNA self-assembly and DNA assembled *via* click chemistry to a pre-formed mixed monolayer. A schematic of DNA monolayer formation *via* copper-free click chemistry is shown in Figure 1.6.

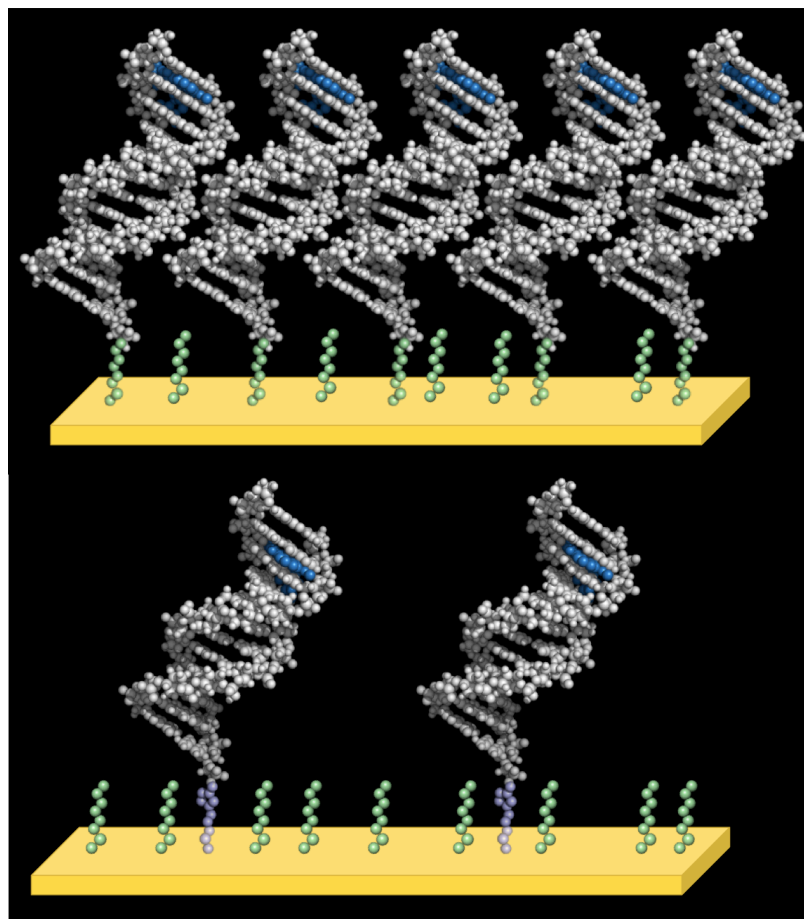


**Figure 1.5** Representation of DNA monolayers formed conventionally and with click chemistry. DNA is shown tethered to a gold electrode surface with a terminally bound redox probe for efficient electrochemical readout. Self-assembled thiolated DNA (*top*) forms regions of very high DNA density, which can prevent access of large biomolecules to the probe sequences on the surface, with other regions of the electrode surface devoid of DNA. In contrast, DNA that is ‘clicked’ onto a pre-formed mixed alkanethiol monolayer has significantly more controlled spacing with more separation between the helices, enabling greater access to the individual probe DNA helices.

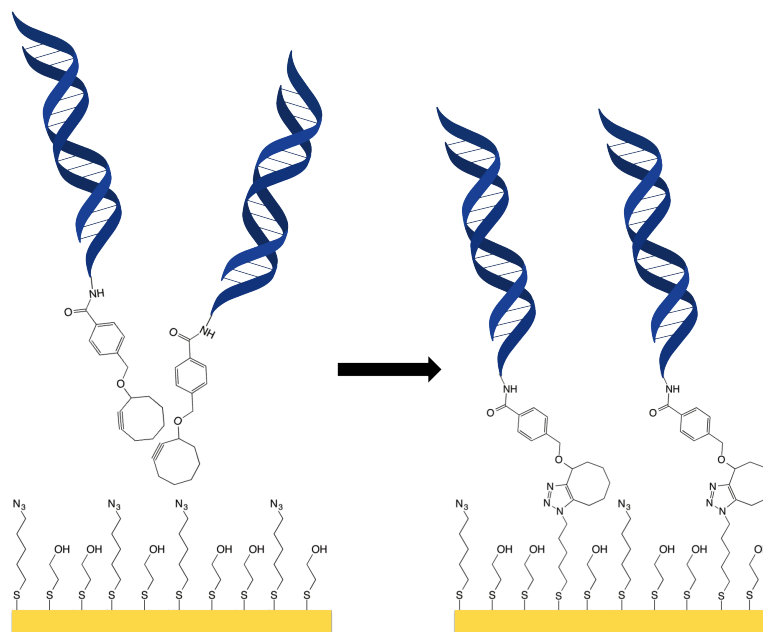


**Figure 1.6** Assembly of DNA monolayers using copper-free click chemistry. DNA modified with a strained cyclooctyne moiety is added to pre-formed mixed alkanethiol monolayers containing ‘active’ azide head groups as well as ‘passivating’ alcohol head groups. The DNA can only attach to the points at which an azide has previously been immobilized. Because of the cyclooctyne ring strain, the reaction between the azide and the alkyne occurs spontaneously.

## Redox Probes for DNA-mediated Charge Transport Detection

Effective detection by DNA CT is dependent on the interaction between a redox probe and the base stack, whether the molecule is covalently tethered to DNA or free in solution. There are multiple modes of non-covalent interaction between small molecules and DNA, including groove binding, electrostatic association, and intercalation. For effective DNA CT, the redox probes must be well coupled into the base pair stack. Intercalation, where the probe is itself  $\pi$ -stacked in the duplex, is a particularly sensitive coupling mode for electrochemical applications. A series of redox-active probes that interact with DNA through either intercalation or groove binding were tested for signal attenuation upon incorporation of a mismatch. The compounds capable of intercalation, including  $[\text{Ir}(\text{bpy})(\text{phen})(\text{phi})]^{3+}$ , daunomycin, and methylene blue, lead to a differential in the electrochemical current between well-matched duplexes and duplexes containing a single-base mismatch. Ruthenium hexammine, however, which is only capable of hydrogen binding in the groove, shows no difference in current between the well-matched and mismatched DNA; here CT is not *through* the base stack. Moreover, the intercalative complexes that are less likely to groove bind,  $[\text{Ir}(\text{bpy})(\text{phen})(\text{phi})]^{3+}$  and daunomycin, have a significantly greater signal differential for mismatch discrimination (CA:TA signal ratio of 0.3) than methylene blue (CA:TA signal ratio of 0.5). Figure 1.7 shows the difference in specificity for mismatch discrimination between the small molecule ruthenium hexammine and the DNA intercalator daunomycin, which speaks to the sensitivity of the  $\pi$ -stack to perturbations to charge transport.

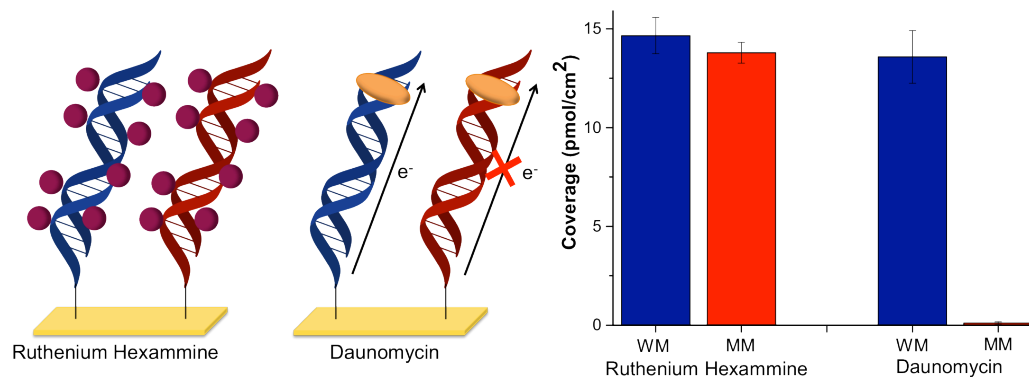


**Figure 1.7** DNA monolayer coverage determined by ruthenium hexammine and daunomycin. Ruthenium hexammine electrostatically interacts with the DNA backbone (purple dots, left), and is therefore a good redox probe to determine the total amount of phosphate on the surface. Daunomycin, a redox-active DNA intercalator, is capable of interacting with the DNA base stack and reporting on perturbations therein (orange spheres, center). When DNA coverage on electrodes is determined by quantifying the redox signal from each of these probes with either well-matched DNA (blue bars, right) or mismatch-containing DNA (red bars, right), ruthenium hexammine yields the same total DNA coverage for both sequences. In contrast, a significant signal attenuation is observed for the daunomycin redox probe with mismatch-containing DNA, as compared to the well-matched sequence.<sup>54</sup>

## Electrocatalysis for Signal Amplification

In order to detect low-abundance species, it may be necessary to amplify the electrochemical signal obtained directly from a DNA-interacting reporter, as these signals can be prohibitively small. To address the problem of small electrochemical signals, an electrocatalytic cycle can be incorporated into the detection platform for signal amplification. The most effective signal amplification system involves intercalated MB coupled to  $\text{Fe}(\text{CN})_6^{3-}$  freely diffusing in solution.<sup>17</sup> Owing to its negative charge, direct electrochemical reduction of  $\text{Fe}(\text{CN})_6^{3-}$  is inhibited at the highly (negatively) charged surfaces of DNA-modified electrodes, even at overpotentials as high as 1 V. On the other hand, reduction of  $\text{Fe}(\text{CN})_6^{3-}$  by leucomethylene blue (LB, the reduced form of MB), is thermodynamically favored by more than 0.5 eV, ensuring a rapid homogeneous electron transfer reaction. Thus, addition of micromolar MB to electrolyte solutions containing millimolar  $\text{Fe}(\text{CN})_6^{3-}$  leads to a dramatic increase in the electrochemical response at a DNA-modified electrode. Importantly, the onset of this response occurs at the reduction potential of MB (indicating MB as the electrochemical mediator), and the reduction is completely irreversible, as the reduced form of MB is oxidized rapidly by  $\text{Fe}(\text{CN})_6^{3-}$  and is therefore no longer available for electrochemical oxidation.

### *Methylene Blue as Electrocatalyst with Ferricyanide*

Based on data collected at rotating disk electrodes,<sup>55</sup> we proposed the mechanism of electrocatalysis between MB and  $\text{Fe}(\text{CN})_6^{3-}$  illustrated in Figure 1.8 for this reaction. The cycle begins with MB intercalated into the DNA film. Upon sweeping the potential past the formal MB/LB reduction potential, MB is rapidly reduced through DNA CT to

LB, which subsequently dissociates from the film and reduces two equivalents of  $\text{Fe(CN)}_6^{3-}$ . Intercalation of regenerated MB back into the film completes the catalytic cycle. The kinetics of this process suggests that the overall catalytic rate is governed by the on/off dynamics of MB/LB into and out of the DNA film. As a consequence, as long as the on/off rates are fast on the electrochemical timescale, the overall current is limited no longer by the surface density of MB in the film, but by the concentration (and diffusion constant) of  $\text{Fe(CN)}_6^{3-}$  in solution. Depending on the concentration of  $\text{Fe(CN)}_6^{3-}$ , this electrocatalysis results in absolute currents that are roughly an order of magnitude higher than those produced by direct electrochemical reduction of MB.

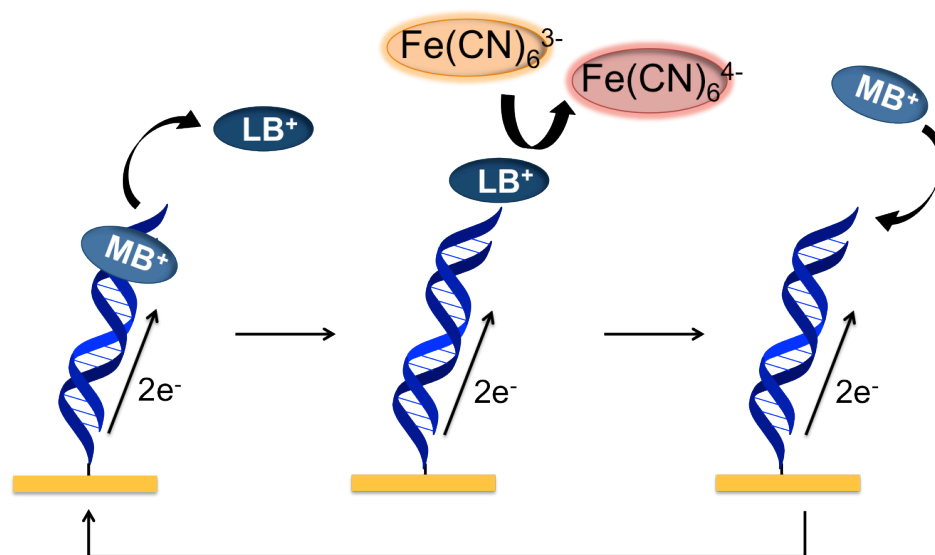


**Figure 1.8** Electrocatalytic cycle between free methylene blue and ferricyanide on a DNA-modified electrode. Methylene blue in its oxidized form is intercalated into the DNA base stack. Upon reduction of methylene blue to leucomethylene blue via DNA-mediated charge transport, the affinity of the leucomethylene blue for DNA is lowered and leucomethylene blue is no longer intercalated. The reduced leucomethylene blue is capable of reducing ferricyanide that is freely diffusing in solution. The leucomethylene blue is then reoxidized to methylene blue and can reintercalate into the DNA. The ferricyanide acts as a diffusing electron sink in solution for the redox probe, methylene blue.



### ***Single Base Mismatch and Lesion Detection with Electrocatalysis***

With a successful catalytic cycle in hand, the question then became whether the presence of a mismatch or other DNA lesion would sufficiently attenuate the catalytic response. Several studies were therefore carried out to assess empirically electrocatalytic signal differentials at well matched versus mismatched helices using a series of different electrochemical mediators. These studies reinforced the importance of selecting redox probes with both the right binding mode and binding kinetics for use in DNA CT electrocatalytic assays. Figure 1.9 illustrates this point by showing the electrochemical response of 1 mM  $\text{Fe}(\text{CN})_6^{3-}$  at well matched and mismatched films in the presence of micromolar concentrations of MB, DM, and  $\text{Ru}(\text{NH}_3)_6^{3+}$ .<sup>55</sup> With relatively fast on/off intercalation dynamics, MB mediates  $\text{Fe}(\text{CN})_6^{3-}$  reduction efficiently at well-matched DNA films, but, because of attenuated DNA CT, yields a dramatically smaller catalytic reduction at films made up of mismatched helices. This differential signal enables MB to serve as a highly effective reporter for DNA base-stack perturbations using electrocatalysis. In contrast, the tightly intercalated DM probe, with very slow on/off dynamics, is unable to mediate  $\text{Fe}(\text{CN})_6^{3-}$  reduction at either type of electrode surface, rendering it unsuitable as an electrocatalyst. Finally, the  $\text{Ru}(\text{NH}_3)_6^{3+}$  probe, which merely ion pairs to the DNA backbone, exhibits the fastest on/off dynamics, and correspondingly mediates the most efficient  $\text{Fe}(\text{CN})_6^{3-}$  reduction. However, because  $\text{Ru}(\text{NH}_3)_6^{3+}$  reduction is not DNA mediated, the electrocatalytic waves are virtually identical at both matched and mismatched films.

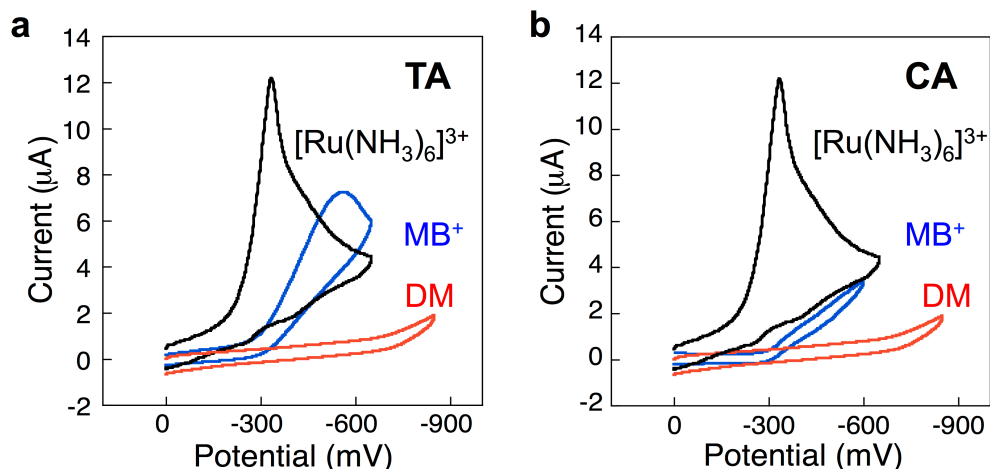


**Figure 1.9** Electrocatalytic signals from DNA-modified electrodes and a variety of redox probes with  $[\text{Fe}(\text{CN})_6]^{3-}$ . In black is the electrocatalytic signal from ruthenium hexammine interacting with  $[\text{Fe}(\text{CN})_6]^{3-}$ ; in blue is freely diffusing methylene blue with  $[\text{Fe}(\text{CN})_6]^{3-}$ , and in red is daunomycin with  $[\text{Fe}(\text{CN})_6]^{3-}$ . In (a) is shown the signals for well-matched DNA, and (b) shows signals for DNA containing a C:A mismatch. As can be seen, no electrocatalytic turnover occurs between daunomycin and  $[\text{Fe}(\text{CN})_6]^{3-}$ , and with ruthenium hexammine, no signal attenuation is observed upon the incorporation of a C:A mismatch. Only methylene blue and  $[\text{Fe}(\text{CN})_6]^{3-}$  produce a DNA mediated signal with electrocatalytic amplification that is attenuated upon incorporation of a mismatch.

Indeed, both the absolute currents for MB-mediated  $\text{Fe}(\text{CN})_6^{3-}$  reduction and, more importantly, the differential currents generated at matched versus mismatched DNA films are an order of magnitude greater than the corresponding currents observed for the direct electrochemical reduction of intercalated MB. Moreover, integrating the steady-state catalytic currents as a function of time yields differential charges at matched versus mismatched films that only get larger with time. This effect is illustrated in Figure 1.10, where the time-dependent electrocatalytic charge is plotted separately for MB-mediated  $\text{Fe}(\text{CN})_6^{3-}$  reduction at films featuring either matched or mismatched DNA helices. Significantly, this chronocoulometry assay allows ready detection of all of the possible single-base mismatches, including purine-purine base steps, without any manipulation of hybridization conditions.<sup>16</sup> The improved signal differentiation as a function of time is a direct consequence of the catalytic nature of this assay.

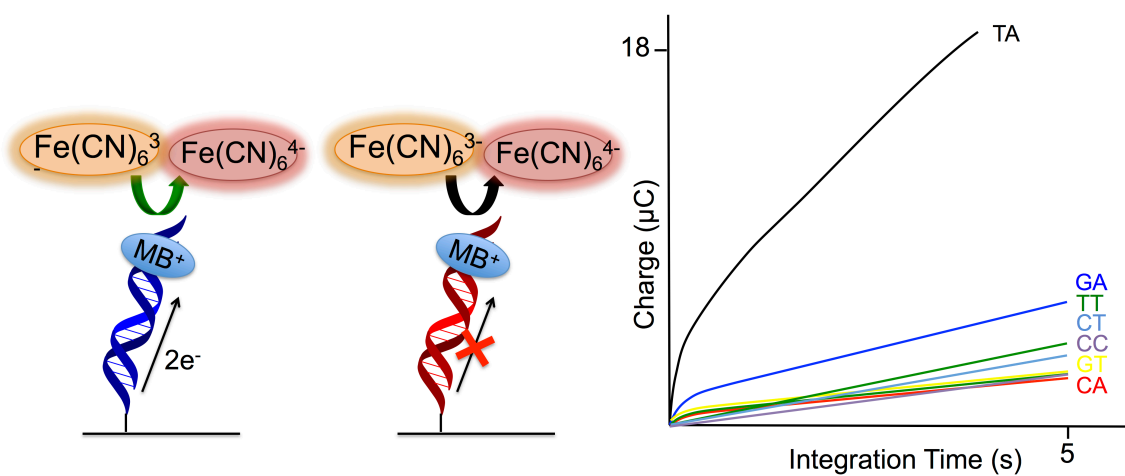


**Figure 1.10** Chronocoulometry of well-matched DNA as well as the same mismatches previously tested with free daunomycin examined with methylene blue and  $[\text{Fe}(\text{CN})_6]^{3-}$ . As can be seen, the difference in charge between well-matched DNA and each of the single base mismatch-containing duplexes is significantly larger for the signals amplified with electrocatalysis than those that do not.

The utility of this electrocatalytic chronocoulometry platform applied to biologically relevant targets was highlighted by the successful detection of different lesion products in DNA, as well as the detection of hot-spot mutations of the human p53 gene.<sup>16</sup> Cellular DNA lesions occur as a result of exposure to reactive-oxygen species and UV light, and this assay proved sufficiently sensitive to differentiate not only between undamaged DNA and DNA containing various lesions but also between the different lesions tested, including an abasic site, 8-oxo-adenine, 5,6-dihydroxy thymine, and deoxy-uracil.<sup>16</sup> Likewise, the assay enabled ready detection of several p53 mutations contained in tumor cell lines using a multiplexed chip featuring microelectrode sensors.<sup>16</sup>

### ***Tethering Methylene Blue***

One drawback of the  $\text{Fe}(\text{CN})_6^{3-}$ -based electrocatalytic system is the stringent requirement for thoroughly passivated electrode surfaces: any direct  $\text{Fe}(\text{CN})_6^{3-}$  reduction at the bare electrode—even at pinholes—bypasses the DNA CT pathway and renders the assay incapable of sensing  $\pi$ -stack perturbations. This is especially problematic when detecting larger biomarkers, *e.g.*, protein transcription factors, which require lower DNA surface densities in order to gain access to specific sequences within the individual helices.<sup>56</sup> Low-density films additionally require that the redox mediator be prohibited from diffusing down into the DNA sequence and intercalating below the site of  $\pi$ -stack disruption.

A method was therefore developed to covalently tether methylene blue directly to the terminus of the DNA. The covalent MB reporter is coupled to a modified thymine base through a flexible molecular tether which maintains the capacity of MB to

intercalate into the DNA base stack and still dissociate upon reduction to LB.<sup>57</sup> In covalent linkage of methylene blue to the DNA, the linker length was of the most concern. The linker must be flexible enough and sufficiently long for the probe to intercalate into the base stack, while not so long that the probe can interact directly with the surface. The length of the tether was optimized to a 6-carbon chain because this length enabled the probe to destack from the bases upon reduction to leucomethylene blue and interact with the diffusing electron sink and to intercalate into the DNA base stack in the oxidized methylene blue form, while being sufficiently short to minimize direct surface interactions between the probe and the gold electrode. Additionally, unlike free methylene blue, with the covalent methylene blue probe, there is only a single redox reporter per DNA helix.

Various tethers for MB have been explored, and it was found that too short a tether did indeed limit access to solution, but a longer linker gave direct interaction with the gold electrode.<sup>57, 58</sup> We also considered whether intercalation was always intraduplex for the tethered probes. Here, clearly the extent of intraduplex intercalation depended upon how closely packed the DNA helices were. Most importantly, an essential element for all these characterizations was the assay for how effective a mismatch served to attenuate current flow. The key for efficient DNA detection was CT mediated by the full helix, as tested through the inclusion of intervening mismatches.

### ***Covalent Methylene Blue with Hemoglobin as an Electrocatalysis Pair***

To address the problem of direct-electrode  $\text{Fe}(\text{CN})_6^{3-}$  reduction, a metalloprotein-based electron sink was additionally employed to provide some inherent shielding from

the electrode surface. While a variety of redox-active proteins have been applied generally to electrocatalytic platforms, including glucose oxidase and horseradish peroxidase, many of these generate undesirable reactive oxygen species.<sup>59-61</sup> Hemoglobin, in contrast, is a fairly small protein that does not generate byproducts that can damage DNA.

Because of the iron center shielding afforded by hemoglobin's native protein conformation, passivation of the DNA-modified electrode is less of a stringent necessity when this protein is used as an electron sink (Figure 1.11).<sup>62</sup> The combination of a covalent MB mediator and hemoglobin electron sink enabled the ready detection of restriction enzyme activity at a low-density DNA film. Notably, using covalent MB and  $\text{Fe}(\text{CN})_6^{3-}$ , detection of DNA was limited to greater than 500 fmol on the surface. In contrast, upon incorporation of hemoglobin, DNA was detectable at 5 fmol on the surface, increasing the sensitivity of detection by 100 fold.

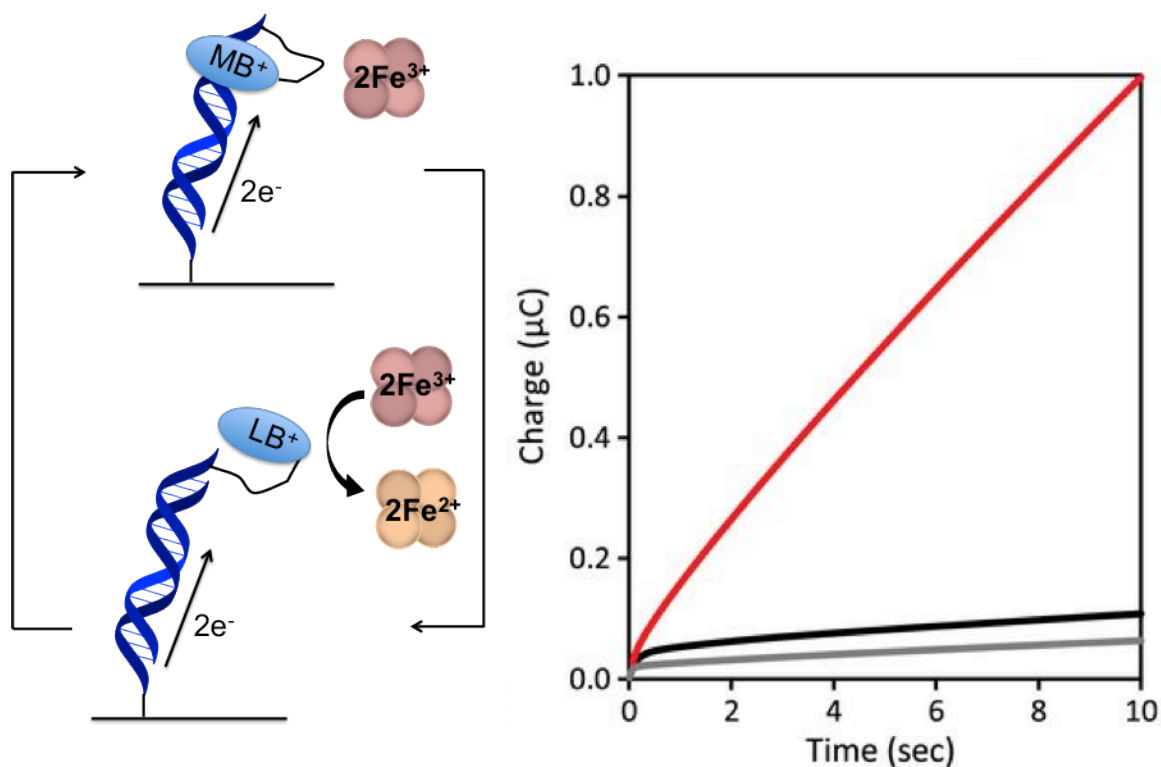


**Figure 1.11** Electrocatalytic cycle between DNA tethered MB and freely-diffusing hemoglobin. As MB is reduced to LB, its affinity for DNA is significantly decreased, resulting in LB dissociation from the duplex. The LB is then reoxidized by hemoglobin in solution while maintaining surface passivation. The amino acids of the hemoglobin shell provide an inherent passivator between the iron center and electrode surface. The chronocoulometry of the system is shown. In red is the signal resulting from electrocatalysis, while in black is the MB-DNA without hemoglobin, and in grey is unmodified DNA duplex.



## Platforms for DNA Electrochemistry

Sensitive detection of biomarkers is necessary for fundamental biological studies as well as for the development of effective diagnostic tools. As DNA can be used to specifically capture DNA, RNA, and proteins, nucleic acid sensors provide a flexible platform that can be easily manipulated to detect a variety of targets. Moreover, their structure is amenable to multiplexed formats.

Many modern DNA sensors involve modifying capture or target nucleic acids with fluorophores and observing changes in fluorescence upon a hybridization event.<sup>63</sup> Because these platforms rely solely on hybridization, probe sequences can be varied in an array that can contain hundreds of thousands of individual DNA sequences in a single square centimeter.<sup>64, 65</sup> While these platforms provide a significant amount of information, such as gene expression levels, and cannot currently be matched in information content with multiplexed electrochemical chips, the fluorescence assays lack the sensitivity and specificity required to directly detect biomarkers at low concentrations for both fundamental biological studies and diagnostic applications. Furthermore, these assays are expensive, require sophisticated instrumentation, and are thus not well suited for point of care diagnostics.

Electrochemically-based DNA platforms are very well suited for diagnostic applications, from the research lab to clinic, as they are generally very simple and sensitive, and do not require the complex labeling of targets.<sup>31</sup> Charge transport offers a powerful means to interrogate and report on the integrity and conformation of the base stack. Traditionally, DNA-modified electrodes are formed from thiolated DNA self-assembled onto a gold surface (Figure 1.4). The gold is then passivated with

mercaptohexanol to minimize direct interactions between redox-active moieties and the electrode surface. DNA CT sensors are based on the flow of electrons from the surface of electrodes through the DNA base stack to redox-active reporters. Importantly, the flow of electrons through DNA is inhibited by anything that perturbs the DNA base stack, including a single base mismatch, as described above, a DNA lesion, or the binding of a protein that disrupts the DNA base stack upon binding, as in proteins that kink DNA or flip bases out of the helix.<sup>66</sup> This sensitivity enables the detection of many classes of biomolecules, from single-stranded DNA to RNA and proteins.<sup>67</sup>

Electrochemical devices utilizing DNA CT have evolved over time. The first DNA CT-based detection platforms contained only a single electrode. This was advantageous, as devices were simple and could be constructed using commercially available materials. However, single-electrode platforms were limited because multiple experimental parameters could not be directly compared, making subtle differences between samples difficult to discern. More complex electrochemical systems have been developed to address this issue. A multiplexed platform allowing for the simultaneous analysis of different experimental conditions on the same chip was developed. The current multiplexed silicon chip is fabricated with 16 individually-addressable gold electrodes divided into four isolated quadrants.<sup>68</sup> This platform has enabled the incorporation of significantly more complex experiments due to the ability to run multiple experimental conditions in parallel.

We have also recently developed a two working electrode platform for sensing, which enables spatial addressing of many sequences of DNA on an electrode through the patterning of multiple sequences of DNA onto a single electrode surface.<sup>69</sup> This two-

electrode setup involves a large substrate electrode onto which DNA can be specifically patterned in an array via site-specific activation of a click catalyst at a secondary electrode. Detection is subsequently performed through scans across the array with a microelectrode to detect DNA-mediated electrochemistry. Through a simple method of fabrication, this platform allows uniformity in arrays as well as highly sensitive, localized detection with spatial resolution.

While patterning multiple DNA sequences onto a single electrode surface enables direct comparisons between those sequences upon treatment with one particular analyte solution, for clinically relevant detection, it may be necessary to detect differences between solutions. We therefore developed a platform that combines our low-density DNA monolayers with the capacity for multiplexing, as with our multiplexed DNA chips.<sup>70</sup> This platform contains two electrode arrays, a primary array to act as a multiplexed DNA-modified substrate, and a secondary array to function as a set of patterning and detection electrodes.

## Detection of Single Base Mutations and DNA Lesions

DNA-modified electrodes thus provide a powerful technique to monitor mismatches in DNA and therefore also genomic mutations. Electrochemical signal attenuation has been shown with every possible base mismatch, irrespective of sequence context.<sup>16, 17</sup> Chronocoulometry, with signal amplification through electrocatalysis of ferricyanide by methylene blue, was used to observe all mismatched base pairs.<sup>16</sup> Purine-purine, pyrimidine-purine, and pyrimidine-pyrimidine mismatches all lead to significantly attenuated signals by electrocatalysis. This chemistry can also be applied to the detection of DNA lesions. The majority of DNA lesions have only a small thermodynamic and structural impact on the DNA helix, making them especially difficult to detect with many platforms. However, similarly to single-base mismatches, lesions disrupt the long-range  $\pi$ -stacking of the bases, making them detectable using DNA CT. With chronocoulometry, many common DNA lesions have been shown to significantly attenuate charge accumulation.<sup>15</sup> These include a hydroxylation product of thymine (5,6-hydroxy thymine), an abasic site, an adenine oxidation product (8-oxo-adenine), and a cytosine deamination product (deoxy-uracil). All lesions tested lead to signal attenuations on the order of those observed for mismatches.

## Detection of DNA-Binding Proteins

DNA CT platforms are similarly advantageous for the detection of proteins that interact with DNA. Here we describe a variety of proteins that bind to DNA in different ways but can all be detected sensitively using DNA electrochemistry.

### *Detection of Transcriptional Regulators*

Transcription factors are vital components of cellular genetic regulation. Transcriptional activators and repressors control the recruitment of RNA polymerase to commence RNA transcription. Many of these proteins primarily interact with DNA simply by bending the helix at the binding site. Because their binding is completely reversible and they do not permanently alter the DNA in any way, transcription factors can be difficult to detect with many DNA-based platforms. However, these proteins can be an important component of pathogenesis, as many influence regulation of tumor suppressor genes or oncogenes, making mutations to the sequences of these proteins potentially extremely deleterious in the cell.<sup>71</sup> As the primary mode of interaction between some of these proteins and DNA is significant helical bending, which distorts the  $\pi$ -stacking of the bases, DNA CT-based detection can be advantageous for their detection.

The transcriptional activator TATA-binding protein (TBP) has been easily detected on DNA-modified electrodes, given the large perturbation in DNA stacking associated with the binding of TBP. TBP binds to a TATA sequence in DNA and kinks the helix 80° at that location, leading to a significant DNA-mediated signal attenuation.<sup>72</sup> Figure 1.12 shows this result.<sup>66</sup> A DNA-modified electrode containing a covalently

bound redox probe shows a large accumulation in charge by chronocoulometry. In the presence of TBP, which binds to the specific 5'-TATA-3' site and kinks the DNA, the charge accumulation is significantly attenuated. Protein binding acts essentially as a switch, turning off DNA CT. In contrast, some proteins that regulate DNA expression bind without perturbing the DNA helix. Helix-turn-helix proteins are one example. These proteins have no significant effect on DNA CT.

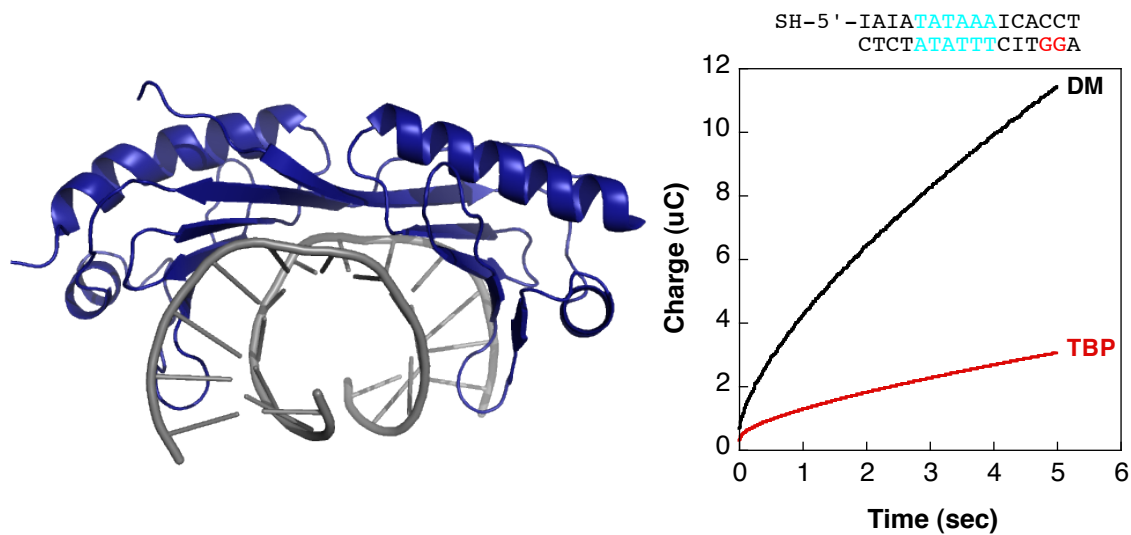


**Figure 1.12** Electrochemistry of DNA with TATA-binding protein (TBP). Left: Illustration of the crystal structure of TBP (blue) bound to DNA (grey);<sup>72</sup> a significant kink in the DNA helix is observable. Right: Chronocoulometry of the DNA-modified electrode without protein (black) and with TBP bound (red).<sup>66</sup> As can be seen, the total charge accumulation in the presence of TBP is significantly smaller than in its absence.

### ***Photolyase Activity and Detection***

Photolyases repair UV damage to DNA, notably pyrimidine-pyrimidine dimers (thymine or cytosine dimers).<sup>73</sup> Thymine dimers ( $T \diamond T$ ) are some of the most common lesions caused by UV damage and greatly distort the structure of DNA. They can result in mutagenesis and are linked to the development of melanomas. Photolyases repair such lesions in bacteria and fungi using visible light and a flavin cofactor. Because thymine dimers disrupt the  $\pi$ -stack, not surprisingly, they attenuate DNA CT. Upon photolyase repair, though, CT is restored through the repaired DNA. This result was shown on DNA-modified electrodes with DNA containing a pre-formed  $T \diamond T$ .<sup>74</sup> Rather than requiring the incorporation of a redox probe, a signal is observed from the flavin cofactor of the protein bound to the DNA. However, this signal is diminished when a  $T \diamond T$  is incorporated. As the protein-DNA complex is irradiated over time, facilitating DNA repair, the electrochemical signal increases and then levels off, consistent with the repair time for photolyase. Repair of photolyase was confirmed by HPLC. Thus, DNA repair by photolyase can be monitored electrochemically.

### ***Methyltransferase and Methylation Detection***

Methyltransferases are proteins responsible for methylation of the genome and are gaining wide interest given their importance in the regulation of gene expression. It has recently been shown that aberrant levels of methyltransferase protein are often early indicators of cancer.<sup>75-77</sup> Methyltransferases generally require the flipping of a base out of the  $\pi$ -stack in order to accomplish methylation; after the methyl group has been successfully added to the nucleotide, the base is returned to the DNA stack.<sup>78</sup> While the



methylated DNA base product does not hinder DNA CT, CT is significantly diminished when the base is flipped out of the  $\pi$ -stack and a non-aromatic protein residue is inserted into the base stack, seemingly as a placeholder for the flipped base while methylation occurs. This signal attenuation upon base flipping was shown through the detection of a methyltransferase on a DNA-modified electrode surface.<sup>66</sup> Interestingly, if a mutant methyltransferase is used in which an aromatic residue is inserted in the stack, no attenuation of CT is evident.

Methyltransferases have additionally been detected using the carbon nanotube devices, and a reduced affinity of the protein for the DNA after methylation was found.<sup>79</sup> When a single DNA helix containing the binding site for *SssI*, a bacterial methyltransferase, was exposed to *SssI* without the necessary cofactor, S-adenosyl methionine (SAM), a small attenuation in the current through the device was observed. However, upon the addition of the cofactor, the current dropped significantly. This decrease in current was attributed to the destacking of the bases, as the protein flips a base out of the  $\pi$ -stack in order for methylation to occur. Restoration of current occurs as the protein is washed from the DNA. Interestingly, given that this corresponds to a single molecule measurement, when the protein was again added to the duplex with its cofactor, no significant current attenuation was observed, as the DNA was already methylated. This result indicates that the affinity of the protein for methylated DNA is significantly lower than for its unmethylated counterpart.

Ideally, however, protein detection is performed with a 'signal-on' system, as many nonspecific events can cause signal attenuation. Such an assay has been developed in which DNA that has been successfully methylated maintains its electrochemical signal,

while DNA that remains unmethylated is cut by a methylation-specific restriction enzyme.<sup>80</sup> This assay has specifically been used for the detection of the human methyltransferase DNMT1 and the bacterial methyltransferase *SssI*. DNMT1 is the methyltransferase responsible for both the establishment and maintenance of cytosine methylation patterns in the human genome. Aberrant methylation patterns caused by underexpression or overexpression of methyltransferases have been linked to the proliferation of cancers. A bacterial methyltransferase, *SssI*, a SAM-dependent protein with a preference for unmethylated DNA, was first used, as *SssI* has significantly higher activity than DNMT1. At 20 nM protein concentration, almost full signal protection is achieved upon addition of the restriction enzyme *BstUI*, which has a preference for unmethylated DNA. When surfaces were treated with either the SAM cofactor alone or the *SssI* protein alone, large signal decreases were observed upon treatment with *BstUI*. The surfaces were then treated with the restriction enzyme *RsaI*, which cuts both unmethylated and hemi-methylated DNA. All quadrants had significant signal decreases upon treatment, establishing that the DNA was hemi-methylated in the presence of *SssI* and SAM (Figure 1.13).

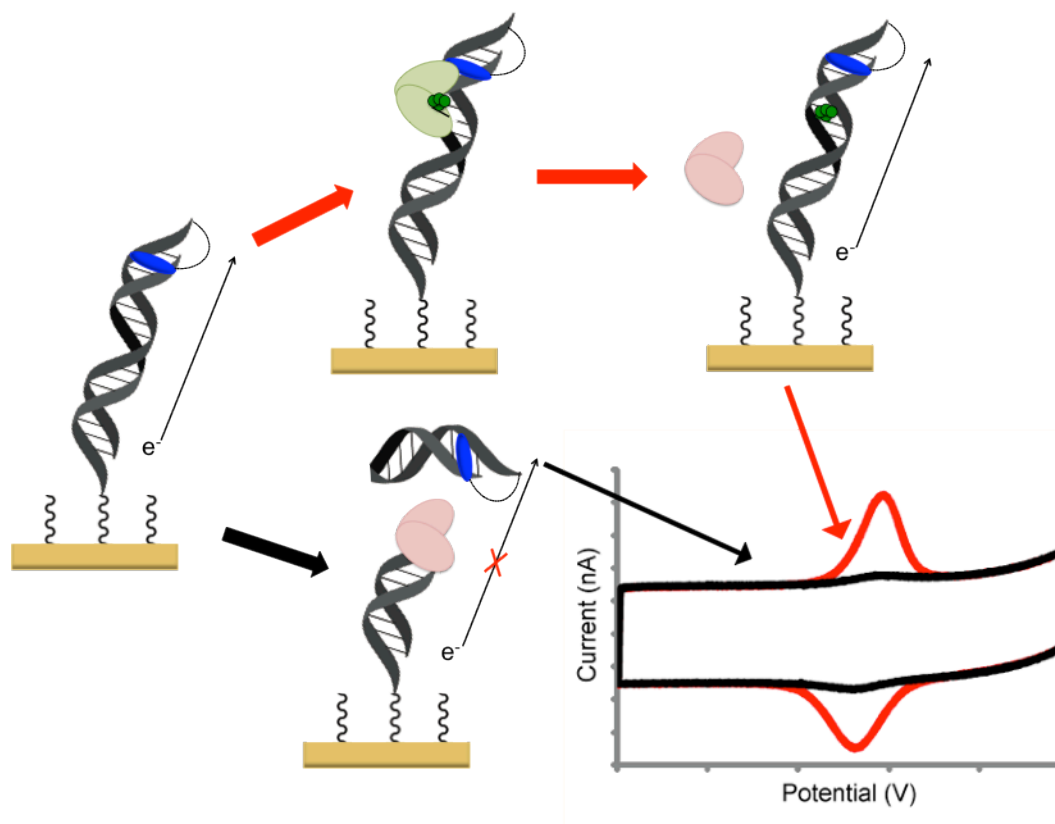


**Figure 1.13** Electrochemical assay for methyltransferase activity. DNA duplexes that either contain a binding site for the methyltransferase protein (red arrow) or does not contain the binding site (black arrow) are assembled on electrodes. Methyltransferase protein (green) and S-adenosyl methionine (SAM) cofactor are added to the surface, and the protein is allowed to methylate the DNA. If the DNA is methylated, restriction enzymes (pink) selective for unmethylated DNA will not cut the DNA, maintaining an 'on' signal (red cyclic voltammogram). If the DNA remains unmethylated, upon addition of the restriction enzyme, the DNA is cleaved (bottom route), and the electrochemical signal turns off (black cyclic voltammogram).<sup>80</sup>

This assay was then tested with the human methyltransferase DNMT1, which only methylates hemi-methylated DNA and is associated with genomic methylation maintenance.<sup>81</sup> In a similar manner to *SssI*, DNMT1 was allowed to methylate DNA on surfaces containing either unmethylated or hemimethylated DNA. *BssHII*, a restriction enzyme that cuts unmethylated or hemimethylated DNA but not fully methylated DNA, duplexes was then added. Hemimethylated surfaces that had DNMT1 and SAM added at protein concentrations as little as 10 nM saw protection from restriction enzyme cutting. Because genomic methylation patterns and the proteins responsible for this are linked to the development of cancers,<sup>82-88</sup> the further development of this assay is vital for the development of early cancer diagnostic tools.

## Conclusions

The ability of DNA to conduct charge is a fascinating and powerful chemistry. Many electrochemical detection platforms have been developed to probe enzymatic activity and the fidelity of DNA. DNA CT can occur over long molecular distances, at least 34 nm, has a shallow distance dependence, and is exquisitely sensitive to perturbations to the DNA helix. The variety of biological elements that have been shown to affect DNA CT, including DNA lesions and mismatches, transcription factors, and proteins containing iron-sulfur clusters, speaks to the potential importance of DNA CT for biosensing applications.

The thesis work described herein utilizes DNA CT-based detection platforms to expand our biological detection capabilities. Chapter 2 describes the application of copper-free click chemistry to better control the density and homogeneity of DNA monolayers. This method of monolayer formation is expanded in Chapter 3 to form patterned DNA arrays. These arrays incorporate a secondary electrode with electrocatalytically-amplified signals for sensitive biomolecule detection. Chapters 4 and 5 describe the multiplexing of this platform to enable sensitive and selective detection of transcription factors and the application of a signal-on method for methyltransferase detection. The combination of the multiplexed, two working electrode platform with the signal-on methyltransferase assay enables detection of methyltransferase activity from tumor samples, which is further investigated for its clinical relevance in Chapter 6. In Chapter 7, the two working electrode platform is applied directly to a flow-through system for microfluidic detection. Finally, efforts toward applications of DNA CT for nanocircuitry are presented in Chapter 8.

This body of work reflects recent advances in DNA CT-based electrochemical sensors that significantly extend detection capabilities. With improvements to both the morphology of DNA monolayers and the methods used for signal amplification, specific protein detection is possible from crude tissue samples. These advances in DNA CT-based platforms have moved this class of sensors from purely academic to clinically relevant.

## References

1. Neidle, S., Puvvada, M. S., and Thurston, D. E. (1994) The relevance of drug DNA sequence specificity to anti-tumour activity, *Eur. J. Cancer*. 30A, 567-568.
2. Watson, J. D., and Crick, F. H. (1953) Molecular structure of nucleic acids; a structure for deoxyribose nucleic acid, *Nature* 171, 737-738.
3. Eley, D. D., and Spivey, D. I. (1962) Semiconductivity of organic substances. Part 9.- Nucleic acid in the dry state, *Trans. Faraday Soc.* 58, 411-415.
4. Genereux, J. C., and Barton, J. K. (2010) Mechanisms for DNA charge transport, *Chem. Rev.* 110, 1642-1662.
5. Murphy, C. J., Arkin, M. R., Jenkins, Y., Ghatlia, N. D., Bossmann, S. H., Turro, N. J., and Barton, J. K. (1993) Long-range photoinduced electron transfer through a DNA helix, *Science* 262, 1025-1029.
6. O'Neill, M. A., Becker, H. C., Wan, C., Barton, J. K., and Zewail, A. H. (2003) Ultrafast dynamics in DNA-mediated electron transfer: base gating and the role of temperature, *Angew. Chem. Int. Ed.* 42, 5896-5900.
7. Wan, C., Fiebig, T., Kelley, S. O., Treadway, C. R., Barton, J. K., and Zewail, A. H. (1999) Femtosecond dynamics of DNA-mediated electron transfer, *Proc. Natl. Acad. Sci. USA* 96, 6014-6019.
8. Hall, D. B., Holmlin, R. E., and Barton, J. K. (1996) Oxidative DNA damage through long-range electron transfer, *Nature* 382, 731-735.
9. Holmlin, R. E., Dandliker, P. J., and Barton, J. K. (1997) Charge Transfer through the DNA Base Stack, *Angew. Chem. Int. Ed.* 36, 2714-2730.
10. Lewis, F. D., Liu, X., Miller, S. E., and Wasielewski, M. R. (1999) Electronic Interactions between  $\pi$ -Stacked DNA Base Pairs and Diphenylacetylene-4,4'-dicarboxamide in Hairpin DNA, *J. Am. Chem. Soc.* 121, 9746-9747.

11. Muren, N. B., Olmon, E. D., and Barton, J. K. (2012) Solution, surface, and single molecule platforms for the study of DNA-mediated charge transport, *Phys. Chem. Chem. Phys.* *14*, 13754-13771.
12. Voityuk, A. A., Rösch, N., Bixon, M., and Jortner, J. (2000) Electronic Coupling for Charge Transfer and Transport in DNA, *J. Phys. Chem. B* *104*, 9740-9745.
13. Sontz, P. A., Muren, N. B., and Barton, J. K. (2012) DNA charge transport for sensing and signaling, *Acc. Chem. Res.* *45*, 1792-1800.
14. Kelley, S. O., Holmlin, R. E., Stemp, E. D. A., and Barton, J. K. (1997) Photoinduced Electron Transfer in Ethidium-Modified DNA Duplexes: Dependence on Distance and Base Stacking, *J. Am. Chem. Soc.* *119*, 9861-9870.
15. Boal, A. K., and Barton, J. K. (2005) Electrochemical detection of lesions in DNA, *Bioconjug. Chem.* *16*, 312-321.
16. Boon, E. M., Ceres, D. M., Drummond, T. G., Hill, M. G., and Barton, J. K. (2000) Mutation detection by electrocatalysis at DNA-modified electrodes, *Nat. Biotechnol.* *18*, 1096-1100.
17. Kelley, S. O., Boon, E. M., Barton, J. K., Jackson, N. M., and Hill, M. G. (1999) Single-base mismatch detection based on charge transduction through DNA, *Nucleic Acids Res.* *27*, 4830-4837.
18. Guo, X., Gorodetsky, A. A., Hone, J., Barton, J. K., and Nuckolls, C. (2008) Conductivity of a single DNA duplex bridging a carbon nanotube gap, *Nat. Nanotechnol.* *3*, 163-167.
19. Sassolas, A., Leca-Bouvier, B. D., and Blum, L. J. (2008) DNA biosensors and microarrays, *Chem. Rev.* *108*, 109-139.
20. Wang, R. E., Zhang, Y., Cai, J., Cai, W., and Gao, T. (2011) Aptamer-based fluorescent biosensors, *Current Med. Chem.* *18*, 4175-4184.
21. Dai, N., and Kool, E. T. (2011) Fluorescent DNA-based enzyme sensors, *Chem. Soc. Rev.* *40*, 5756-5770.



22. Dai, N., Guo, J., Teo, Y. N., and Kool, E. T. (2011) Protease probes built from DNA: multispectral fluorescent DNA-peptide conjugates as caspase chemosensors, *Angew. Chem. Int. Ed.* 50, 5105-5109.
23. Epstein, J. R., Leung, A. P., Lee, K. H., and Walt, D. R. (2003) High-density, microsphere-based fiber optic DNA microarrays, *Biosens. Bioelectron.* 18, 541-546.
24. Steel, A. B., Herne, T. M., and Tarlov, M. J. (1998) Electrochemical quantitation of DNA immobilized on gold, *Anal. Chem.* 70, 4670-4677.
25. Steel, A. B., Herne, T. M., and Tarlov, M. J. (1999) Electrostatic interactions of redox cations with surface-immobilized and solution DNA, *Bioconjug. Chem.* 10, 419-423.
26. Caruso, F., Rodda, E., Furlong, D. N., Niikura, K., and Okahata, Y. (1997) Quartz crystal microbalance study of DNA immobilization and hybridization for nucleic Acid sensor development, *Anal. Chem.* 69, 2043-2049.
27. Wang, J., Nielsen, P. E., Jiang, M., Cai, X., Fernandes, J. R., Grant, D. H., Ozsoz, M., Beglieter, A., and Mowat, M. (1997) Mismatch-sensitive hybridization detection by peptide nucleic acids immobilized on a quartz crystal microbalance, *Anal. Chem.* 69, 5200-5202.
28. Liss, M., Petersen, B., Wolf, H., and Prohaska, E. (2002) An aptamer-based quartz crystal protein biosensor, *Anal. Chem.* 74, 4488-4495.
29. Tang, W., Wang, D., Xu, Y., Li, N., and Liu, F. (2012) A self-assembled DNA nanostructure-amplified quartz crystal microbalance with dissipation biosensing platform for nucleic acids, *Chem. Commun.* 48, 6678-6680.
30. Fritz, J., Baller, M. K., Lang, H. P., Rothuizen, H., Vettiger, P., Meyer, E., Guntherodt, H., Gerber, C., and Gimzewski, J. K. (2000) Translating biomolecular recognition into nanomechanics, *Science* 288, 316-318.
31. Drummond, T. G., Hill, M. G., and Barton, J. K. (2003) Electrochemical DNA sensors, *Nat. Biotechnol.* 21, 1192-1199.

32. Odenthal, K. J., and Gooding, J. J. (2007) An introduction to electrochemical DNA biosensors, *Analyst* 132, 603-610.
33. Palecek, E. (1960) Oscillographic polarography of highly polymerized deoxyribonucleic acid, *Nature* 188, 656-657.
34. Singhal, P., and Kuhr, W. G. (1997) Ultrasensitive voltammetric detection of underivatized oligonucleotides and DNA, *Anal. Chem.* 69, 4828-4832.
35. Yang, I. V., and Thorp, H. H. (2001) Modification of indium tin oxide electrodes with repeat polynucleotides: electrochemical detection of trinucleotide repeat expansion, *Anal. Chem.* 73, 5316-5322.
36. Palecek, E., Fojta, M., and Jelen, F. (2002) New approaches in the development of DNA sensors: hybridization and electrochemical detection of DNA and RNA at two different surfaces, *Bioelectrochem.* 56, 85-90.
37. Lucarelli, F., Tombelli, S., Minunni, M., Marrazza, G., and Mascini, M. (2008) Electrochemical and piezoelectric DNA biosensors for hybridisation detection, *Anal. Chim. Acta* 609, 139-159.
38. Yang, W., and Lai, R. Y. (2011) Comparison of the stem-loop and linear probe-based electrochemical DNA sensors by alternating current voltammetry and cyclic voltammetry, *Langmuir* 27, 14669-14677.
39. Rosi, N. L., and Mirkin, C. A. (2005) Nanostructures in biodiagnostics, *Chem. Rev.* 105, 1547-1562.
40. Xia, F., White, R. J., Zuo, X., Patterson, A., Xiao, Y., Kang, D., Gong, X., Plaxco, K. W., and Heeger, A. J. (2010) An electrochemical supersandwich assay for sensitive and selective DNA detection in complex matrices, *J. Am. Chem. Soc.* 132, 14346-14348.
41. Zuo, X., Xiao, Y., and Plaxco, K. W. (2009) High specificity, electrochemical sandwich assays based on single aptamer sequences and suitable for the direct detection of small-molecule targets in blood and other complex matrices, *J. Am. Chem. Soc.* 131, 6944-6945.

42. Umek, R. M., Lin, S. W., Vielmetter, J., Terbrueggen, R. H., Irvine, B., Yu, C. J., Kayyem, J. F., Yowanto, H., Blackburn, G. F., Farkas, D. H., and Chen, Y. P. (2001) Electronic detection of nucleic acids: a versatile platform for molecular diagnostics, *J. Mol. Diagn.* 3, 74-84.
43. Kelley, S. O., Jackson, N. M., Hill, M. G., and Barton, J. K. (1999) Long-Range Electron Transfer through DNA Films, *Angew. Chem. Int. Ed.* 38, 941-945.
44. Slinker, J. D., Muren, N. B., Renfrew, S. E., and Barton, J. K. (2011) DNA charge transport over 34 nm, *Nat. Chem.* 3, 228-233.
45. Kelley, S. O., Barton, J. K., Jackson, N. M., and Hill, M. G. (1997) Electrochemistry of methylene blue bound to a DNA-modified electrode, *Bioconjug. Chem.* 8, 31-37.
46. Herne, T. M., and Tarlov, M. J. (1997) Characterization of DNA Probes Immobilized on Gold Surfaces, *J. Am. Chem. Soc.* 119, 8916-8920.
47. Hobara, D., Sasaki, T., Imabayashi, S.-i., and Kakiuchi, T. (1999) Surface Structure of Binary Self-Assembled Monolayers Formed by Electrochemical Selective Replacement of Adsorbed Thiols, *Langmuir* 15, 5073-5078.
48. Gorodetsky, A. A., Hammond, W. J., Hill, M. G., Slowinski, K., and Barton, J. K. (2008) Scanning electrochemical microscopy of DNA monolayers modified with Nile Blue, *Langmuir* 24, 14282-14288.
49. Peterson, A. W., Heaton, R. J., and Georgiadis, R. M. (2001) The effect of surface probe density on DNA hybridization, *Nucleic Acids Res.* 29, 5163-5168.
50. Lapierre, M. A., O'Keefe, M., Taft, B. J., and Kelley, S. O. (2003) Electrocatalytic detection of pathogenic DNA sequences and antibiotic resistance markers, *Anal. Chem.* 75, 6327-6333.
51. Kelley, S. O., Mirkin, C. A., Walt, D. R., Ismagilov, R. F., Toner, M., and Sargent, E. H. (2014) Advancing the speed, sensitivity and accuracy of biomolecular detection using multi-length-scale engineering, *Nat. Nanotechnol.* 9, 969-980.
52. Bin, X., Sargent, E. H., and Kelley, S. O. (2010) Nanostructuring of sensors determines the efficiency of biomolecular capture, *Anal. Chem.* 82, 5928-5931.

53. Das, J., and Kelley, S. O. (2013) Tuning the bacterial detection sensitivity of nanostructured microelectrodes, *Anal. Chem.* **85**, 7333-7338.
54. Furst, A. L., Hill, M. G., and Barton, J. K. (2013) DNA-modified electrodes fabricated using copper-free click chemistry for enhanced protein detection, *Langmuir* **29**, 16141-16149.
55. Boon, E. M., Barton, J. K., Bhagat, V., Nersissian, M., Wang, W., and Hill, M. G. (2003) Reduction of Ferricyanide by Methylene Blue at a DNA-Modified Rotating-Disk Electrode, *Langmuir* **19**, 9255-9259.
56. Pheaney, C. G., Arnold, A. R., Grodick, M. A., and Barton, J. K. (2013) Multiplexed electrochemistry of DNA-bound metalloproteins, *J. Am. Chem. Soc.* **135**, 11869-11878.
57. Pheaney, C. G., and Barton, J. K. (2012) DNA electrochemistry with tethered methylene blue, *Langmuir* **28**, 7063-7070.
58. Pheaney, C. G., and Barton, J. K. (2013) Intraduplex DNA-mediated electrochemistry of covalently tethered redox-active reporters, *J. Am. Chem. Soc.* **135**, 14944-14947.
59. Ju, H., and Shen, C. (2001) Electrocatalytic Reduction and Determination of Dissolved Oxygen at a Poly(nile blue) Modified Electrode, *Electroanalysis* **13**, 789-793.
60. Pelossof, G., Tel-Vered, R., Elbaz, J., and Willner, I. (2010) Amplified biosensing using the horseradish peroxidase-mimicking DNAzyme as an electrocatalyst, *Anal. Chem.* **82**, 4396-4402.
61. Xu, J.-Z., Zhu, J.-J., Wu, Q., Hu, Z., and Chen, H.-Y. (2003) An Amperometric Biosensor Based on the Coimmobilization of Horseradish Peroxidase and Methylene Blue on a Carbon Nanotubes Modified Electrode, *Electroanalysis* **15**, 219-224.
62. Pheaney, C. G., Guerra, L. F., and Barton, J. K. (2012) DNA sensing by electrocatalysis with hemoglobin, *Proc. Natl. Acad. Sci. USA* **109**, 11528-11533.

63. Heller, M. J. (2002) DNA microarray technology: devices, systems, and applications, *Annu. Rev. Biomed. Eng.* 4, 129-153.
64. Behr, M. A., Wilson, M. A., Gill, W. P., Salamon, H., Schoolnik, G. K., Rane, S., and Small, P. M. (1999) Comparative genomics of BCG vaccines by whole-genome DNA microarray, *Science* 284, 1520-1523.
65. Schena, M., Shalon, D., Davis, R. W., and Brown, P. O. (1995) Quantitative monitoring of gene expression patterns with a complementary DNA microarray, *Science* 270, 467-470.
66. Boon, E. M., Salas, J. E., and Barton, J. K. (2002) An electrical probe of protein-DNA interactions on DNA-modified surfaces, *Nat. Biotechnol.* 20, 282-286.
67. Gorodetsky, A. A., Buzzeo, M. C., and Barton, J. K. (2008) DNA-mediated electrochemistry, *Bioconjug. Chem.* 19, 2285-2296.
68. Slinker, J. D., Muren, N. B., Gorodetsky, A. A., and Barton, J. K. (2010) Multiplexed DNA-modified electrodes, *J. Am. Chem. Soc.* 132, 2769-2774.
69. Furst, A., Landefeld, S., Hill, M. G., and Barton, J. K. (2013) Electrochemical patterning and detection of DNA arrays on a two-electrode platform, *J. Am. Chem. Soc.* 135, 19099-19102.
70. Furst, A. L., Muren, N. B., Hill, M. G., and Barton, J. K. (2014) Label-free electrochemical detection of human methyltransferase from tumors, *Proc. Natl. Acad. Sci. USA* 111, 14985-14989.
71. Darnell, J. E., Jr. (2002) Transcription factors as targets for cancer therapy, *Nat. Rev. Cancer* 2, 740-749.
72. Juo, Z. S., Chiu, T. K., Leiberman, P. M., Baikalov, I., Berk, A. J., and Dickerson, R. E. (1996) How proteins recognize the TATA box, *J. Mol. Biol.* 261, 239-254.
73. Sancar, A. (2008) Structure and function of photolyase and in vivo enzymology: 50th anniversary, *J. Biol. Chem.* 283, 32153-32157.

74. DeRosa, M. C., Sancar, A., and Barton, J. K. (2005) Electrically monitoring DNA repair by photolyase, *Proc. Natl. Acad. Sci. USA* 102, 10788-10792.
75. Brueckner, B., Kuck, D., and Lyko, F. (2007) DNA methyltransferase inhibitors for cancer therapy, *Cancer J.* 13, 17-22.
76. Ghoshal, K., and Bai, S. (2007) DNA methyltransferases as targets for cancer therapy, *Drugs Today* 43, 395-422.
77. Robertson, K. D. (2001) DNA methylation, methyltransferases, and cancer, *Oncogene* 20, 3139-3155.
78. Smith, S. S., Kaplan, B. E., Sowers, L. C., and Newman, E. M. (1992) Mechanism of human methyl-directed DNA methyltransferase and the fidelity of cytosine methylation, *Proc. Natl. Acad. Sci. USA* 89, 4744-4748.
79. Wang, H., Muren, N. B., Ordinario, D., Gorodetsky, A. A., Barton, J. K., and Nuckolls, C. (2012) Transducing methyltransferase activity into electrical signals in a carbon nanotube-DNA device, *Chem. Sci.* 3, 62-65.
80. Muren, N. B., and Barton, J. K. (2013) Electrochemical assay for the signal-on detection of human DNA methyltransferase activity, *J. Am. Chem. Soc.* 135, 16632-16640.
81. Pradhan, S., Bacolla, A., Wells, R. D., and Roberts, R. J. (1999) Recombinant human DNA (cytosine-5) methyltransferase. I. Expression, purification, and comparison of de novo and maintenance methylation, *J. Biol. Chem.* 274, 33002-33010.
82. De Marzo, A. M., Marchi, V. L., Yang, E. S., Veeraswamy, R., Lin, X., and Nelson, W. G. (1999) Abnormal regulation of DNA methyltransferase expression during colorectal carcinogenesis, *Cancer Res.* 59, 3855-3860.
83. el-Deiry, W. S., Nelkin, B. D., Celano, P., Yen, R. W., Falco, J. P., Hamilton, S. R., and Baylin, S. B. (1991) High expression of the DNA methyltransferase gene characterizes human neoplastic cells and progression stages of colon cancer, *Proc. Natl. Acad. Sci. USA* 88, 3470-3474.
84. Esteller, M. (2007) Cancer epigenomics: DNA methylomes and histone-modification maps, *Nat. Rev. Genet.* 8, 286-298.

85. Esteller, M. (2008) Epigenetics in cancer, *New Engl. J. Med.* 358, 1148-1159.
86. Esteller, M., Corn, P. G., Baylin, S. B., and Herman, J. G. (2001) A gene hypermethylation profile of human cancer, *Cancer Res.* 61, 3225-3229.
87. Esteller, M., Fraga, M. F., Paz, M. F., Campo, E., Colomer, D., Novo, F. J., Calasanz, M. J., Galm, O., Guo, M., Benitez, J., and Herman, J. G. (2002) Cancer epigenetics and methylation, *Science* 297, 1807-1808; discussion 1807-1808.
88. Frigola, J., Song, J., Stirzaker, C., Hinshelwood, R. A., Peinado, M. A., and Clark, S. J. (2006) Epigenetic remodeling in colorectal cancer results in coordinate gene suppression across an entire chromosome band, *Nat. Genet.* 38, 540-549.